JOURNAL OF ELECTRON SPECTROSCOPY and Related Phenomena

ELSEVIER Journal of Electron Spectroscopy and Related Phenomena 114–116 (2001) 623–627

www.elsevier.nl/locate/elspec

A photoemission investigation of the superconducting gap in an electron-doped cuprate superconductor

N.P. Armitage[a,*], D.H. Lu[a], C. Kim[a], A. Damascelli[a], K.M. Shen[a], F. Ronning[a], Z.-X. Shen[a], Y. Onose[b], Y. Taguchi[b], Y. Tokura[b]

[a]*Department of Physics, Applied Physics and Stanford Synchrotron Radiation Lab., Stanford University, Stanford, CA 94305, USA*
[b]*Department of Applied Physics, The University of Tokyo, Tokyo 113-8656, Japan*

Received 8 August 2000; received in revised form 14 September 2000; accepted 18 September 2000

Abstract

We have performed angle resolved photoelectron spectroscopy (ARPES) on the electron-doped cuprate superconductor $Nd_{1.85}Ce_{0.15}CuO_4$. Evidence is found for an anisotropic superconducting gap that is consistent with the existence of a d-wave superconducting order parameter in the n-type cuprate superconductors. © 2001 Elsevier Science B.V. All rights reserved.

Keywords: Photoemission; Neodymium; Cuprate; Superconductors; Electron doped; Gap

1. Introduction

$Nd_{2-x}Ce_xCuO_4$ is one of a few electron doped cuprate superconductors [1]. The undoped material is an antiferromagnetic insulator. With the substitution of tetravalent Ce for trivalent Nd, the Neel temperature rapidly drops around $x=0.13$, with superconductivity occurring between $0.14<x<0.18$ for oxygen reduced samples. As compared to the hole doped materials, the antiferromagnetic phase persists to much higher doping levels with superconductivity occuring in a doping range that is narrower by a factor of almost five.

$Nd_{2-x}Ce_xCuO_4$ and other electron doped cuprate superconductors show very different behavior as compared to the p-type materials; transport measurements seem to indicate a more conventional normal state that is reminiscent of Fermi liquid behavior (ρ is linear in T^2 vs. linear in T) [2]; there is evidence for both electron and hole charge carriers in the temperature dependence of the Hall coefficient [3–5]; the incommensurate neutron scattering peak that is seen in the hole doped cuprates appears to be absent in $Nd_{2-x}Ce_xCuO_4$ [6,7].

There is circumstantial evidence for some kind of nearly isotropic superconducting gap of BCS magnitude from Raman [8], tunneling [9], optical [10], and microwave experiments [11,12]. These results are at odds with the more recent tri-crystal experiment that suggests d-wave pairing [13], but consistent with the lack of a zero-bias tunneling peak on the (110) surface [14,15].

ARPES's unique capability of measuring the spectral function of a solid state material as a function of momentum has played an important role

*Corresponding author. Tel.: +1-650-725-5457; fax: +1-650-724-4700.

PII: S0368-2048(00)00258-9

in the cuprate superconductor problem, including the imaging of an anisotropic superconducting gap [16]. However as with other techniques, the vast majority of these measurements have focused on the hole doped materials. The very limited data on $Nd_{2-x}Ce_xCuO_4$ has yielded important information about the existence of a Fermi surface that has a size roughly consistent with its expected Luttinger volume, the semblance of bands that appear to shift rigidly upon doping, and the existence of an extended flat band at (π, 0) that, unlike the near E_f feature found in the p-type cuprates, is located approximately 300 meV below E_f [17,18]. Previous instrumentation limitations gave energy (150 meV) and momentum resolution (10% of the typical Brillouin zone size) that was too poor to do more detailed analysis or investigation.

2. Experimental

Single crystals of $Nd_{1.85}Ce_{0.15}CuO_4$ were grown by the traveling solvent floating zone method in 4 atm of O_2. The *c*-axis lattice constant agrees well with previously reported values confirming the desired Ce concentration. As-grown boules are not superconducting and must be post-growth annealed to remove the apical oxygen that can exist as impurities in the T' structure [19]. Both resistivity and magnetic susceptibility measurements show an onset of the superconducting transition at 25 K. A superconducting volume (Meissner shielding) of almost 100% at 20 K is a testament to their extremely high quality.

Recent advances in photoelectron spectroscopy are allowing for unprecedented energy and momentum resolution. The possibility of energy resolution on the order of 10 meV and angular resolution $<0.5°$ makes $Nd_{1.85}Ce_{0.15}CuO_4$ an ideal system for reinvestigation and the investigation of its superconducting gap a real possibility. These ARPES measurements were performed at the newly commissioned beamline 5-4 of the Stanford Synchrotron Radiation Laboratory. This system is a Scienta SES 200 electron spectrometer coupled to a normal incidence monochromator (NIM). Samples are positioned by a custom dual axis sample manipulator that can be cooled below 10 K.

We took high resolution angle resolved cuts at two temperatures through $\mathbf{k_F}$ points in two different regions of momentum space (near ($\pi/2$, $\pi/2$) and (π, 0.3π)) as shown in the insets to Fig. 1. In both cases the photon energy was 16.5 eV, the polarization was parallel to the cut direction, and the energy resolution was 11 meV. Chamber pressure was lower than 4×10^{-11} Torr. Samples were cleaved in situ at 10 K which resulted in shiny flat surfaces of which LEED shows them clean and well-ordered with a symmetry commensurate with the bulk. Angle integrated photoemission reveal a large well formed valence band and a near E_f foot. All angle resolved measurements were performed on this foot. ARPES

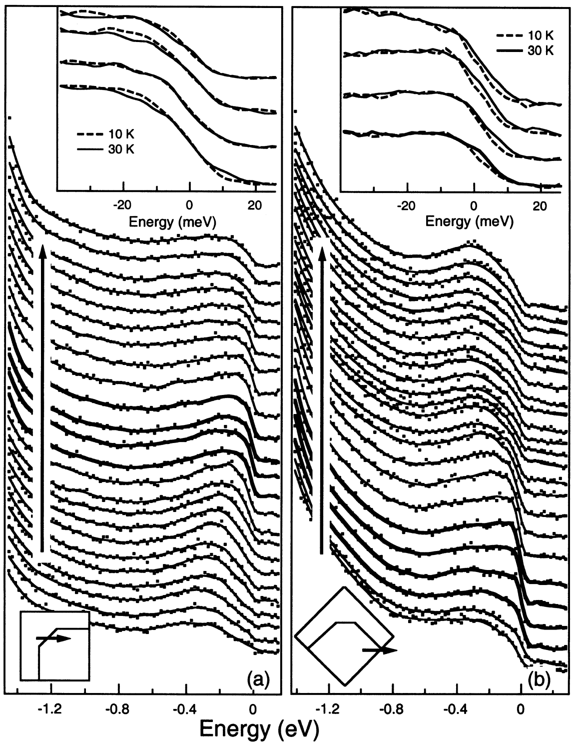

Fig. 1. Energy distribution curves (EDCs) from a $\pm5.5°$ angular windows ($\pm21\%$ π/a) near ($\pi/2$, $\pi/2$) and (π, 0.3π), respectively. In the insets we compare EDCs taken at 30 K (bold) and 10 K (dashed) from near the $\mathbf{k_F}$ positions (represented by the darker curves in the main panels). A clear temperature dependent shift is seen near (π, 0.3π) whereas there is little if any near ($\pi/2$, $\pi/2$). Arrows denote the direction that angular cuts are displayed as referenced to the arrows in insets of the Brillouin zone.

spectra did not change for duration of the experiment ($\simeq$24 h) and were reproduced on a large number of samples.

3. Results

When a material undergoes a superconducting transition, an energy gap opens in the single particle excitation channel in regions along the Fermi surface. This energy gap is responsible for the remarkable stability of the superconducting state. In the phonon mediated BCS model the gap opens more or less isotropically. As pointed out above, the d-wave superconductors have an anisotropic gap, which is a manifestation of a momentum dependent order parameter with positive and negative lobes and nodes in between. In a photoemission experiment one would expect to see a gap in the spectral weight at the Fermi energy along certain regions of the Fermi surface. In reality the clean gap is broadened by instrumental resolution and partially obscured by a large background that may or may not be gapped itself. We can take as a very approximate measure of the gap the midpoint of the leading edge (LEM) of the onset of spectral weight as referenced to the *Fermi energy.* Due to finite instrument resolution, there is some uncertainty in the absolute magnitude of the superconducting gap, but as long as the overall systematics of the lineshape do not change greatly, this analysis is very sensitive to changes in the gap magnitude. A gap in Bi2212, $La_{1.85}Sr_{0.15}CuO_4$, and $YBa_2Cu_3O_{7-x}$ has been found that follows the d-wave functional form [20–22].

This kind of analysis is not reliable in the small gap n-type systems, as a consequence of the fact that the superconducting gap by any measure is much smaller than in the hole doped materials and hence is obscured due to finite resolution and subtle changes in the lineshape around the Fermi surface. In this case, due to a second component that appears near (π, 0) (detailed below) the systematics of the lineshape do change and a simple comparison with E_F is not valid even to measure relative changes in the intrinsic leading edge displacement. It is then crucial that one compare leading edge midpoints (LEMs) above and below T_c at the same momentum space point on the same sample in order to accurately measure the gap value.

In Fig. 1a and b, we present energy distribution curves (EDCs) of the spectral function in a $\pm 5.5°$ ($\pm 21\%$ π/a)angular windows from the cuts near ($\pi/2$, $\pi/2$) and (π, 0.3π) in the directions shown in the Brillouin zone schematics. In the spectra near ($\pi/2$, $\pi/2$) we find a dispersion which is universal for the cuprates in this region of the Brillouin zone. A large broad feature disperses towards the Fermi energy, sharpens, and then disappears as it passes above E_F. In Fig. 1b, which is a cut through $\mathbf{k_F}$ at approximately (π, 0.3π), the spectra are best characterized by a large hump feature that disperses only slightly while the smaller low energy feature disperses toward E_F, loses weight, and then disappears. This behavior has been characterized in more depth elsewhere [23]. Here, we focus on the change in the near $\mathbf{k_F}$ spectra at E_F as a function of temperature, as the onset of superconductivity opens a gap below T_c. In the insets to Fig. 1, we compare spectra taken at 30 K (bold) and 10 K (dashed) at a few near $\mathbf{k_F}$ positions for each cut. In the inset to Fig. 1a from the spectra near ($\pi/2$, $\pi/2$) we see that, aside from some small thermal broadening, there is no temperature induced change. This is quite different from that of spectra from the $\mathbf{k_F}$ crossing near (π, 0.3π) where there is a systematic displacement by ~1.5–2 meV of the leading edge to higher binding energy in the superconducting state.

In Fig. 2 there is an enlarged image of a spectrum with one of the large temperature induced shifts in Fig. 1b. To more systematically quantify the result, we fit the lineshape with a simple phenomenological model. We approximate the superconducting state spectra by a 10 K Fermi function multiplied by a linear spectral function whose onset edge is displaced from the Fermi energy by the superconducting gap energy. We model the normal state spectra as that of a 30 K Fermi distribution at finite temperature multiplied by the same (but non-displaced) linear spectral function. These model spectra are convolved with a Gaussian of FWHM of 11 meV to simulate the experimental resolution. Both the model spectral functions and their convolutions are shown in Fig. 2. The agreement between the experimental curves and the fits are quite good within this picture with a gap parameter of 1.9 meV. This model is only meant to

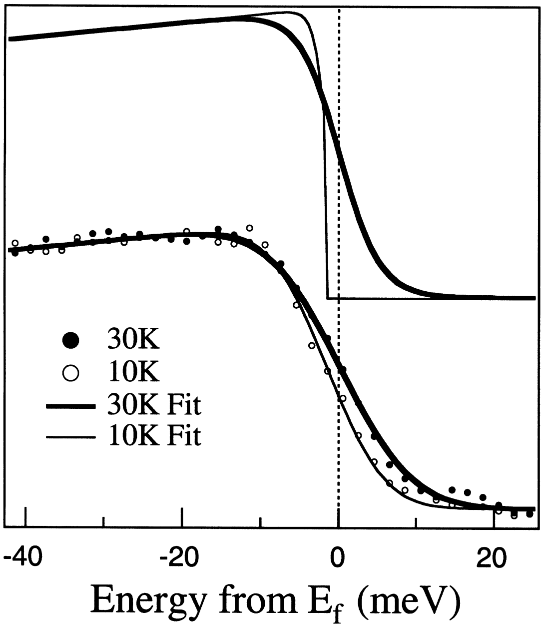

Fig. 2. At the bottom of the panel are EDCs from $\mathbf{k_F}$ near (π, 0.3π) taken from Fig. 1. They are plotted along with a simple fit convolved with the resolution. At the top is the same fit unconvolved with the experimental resolution. The fitted gap parameter is 1.9 meV.

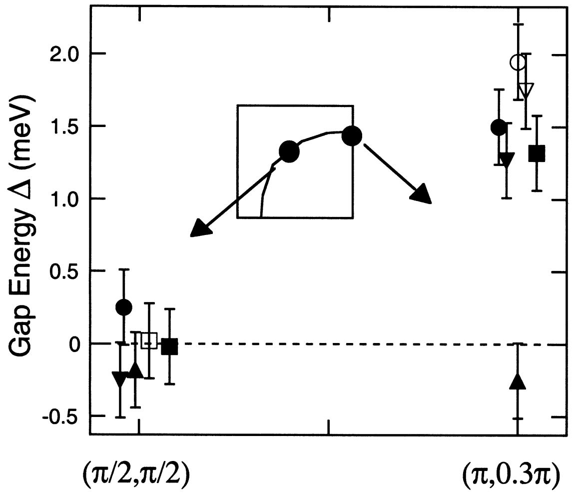

Fig. 3. A plot of all the temperature dependence data taken near ($\pi/2$, $\pi/2$) and (π, 0.3π). The data are slightly offset from each other in the horizontal direction for display purposes. The inset is a schematic indicating the approximate points that data was taken in $\mathbf{k}$-space.

give a systematic bias-free method of quantifying the LEM and we make no claim that it represents the intrinsic spectral function.

The above temperature dependent measurements were repeated on seven different samples (four samples at both $\mathbf{k_F}$ positions, two only at (π, 0.3π) and one just at ($\pi/2$, $\pi/2$)). In Fig. 3 we plot the temperature dependent shift of the LEM at both $\mathbf{k_F}$ crossings for all samples. Although there is some scatter in the data, one can see that, with the exception of one sample, they all show a 1.5–2 meV shift at the (π, 0.3π) position and a negligible one at the ($\pi/2$, $\pi/2$) position. This shift anisotropy is interpreted as a consequence of the opening of a superconducting gap that is maximal near (π, 0) and minimal or zero along the zone diagonal. This is consistent with the presence of a $d_{x^2-y^2}$ superconducting order parameter. The reason for the lack of a temperature dependent shift on the one sample is unknown. Its spectral features and dispersions were consistent with the others. It is possible that it suffered from being in poor thermal contact with the cold stage.

4. Discussion

The obtained maximum gap value of 1.5–2 meV is consistent with, but slightly smaller than, the gap values reported by other techniques [8–12]. There are a few possibilities for this. These other measurements typically take place at 4.2 K (0.15 T_c), in contrast to our measurement at approximately 0.5 T_c. At our intermediate temperatures the superconducting gap may not have fully opened. In addition, there may be some background contribution to the spectra that partially obscures the gap signal. Lastly, it is well documented that photoemission analysis based on LEMs consistently underestimates the maximum gap value (in some cases by as much as a factor of two) as compared to the intrinsic value defined as the quasiparticle peak position [20].

5. Conclusions

In conclusion, we find a momentum anisotropy in the temperature dependence of the ARPES spectra in $Nd_{1.85}Ce_{0.15}CuO_4$. A shift is observed in the low energy spectra near (π, 0) that is consistent with the opening of a 1.5–2 meV superconducting gap. This contrasts with the behavior near ($\pi/2$, $\pi/2$) which shows a negligible temperature dependence. We believe this is evidence for a anistropic superconducting gap in the electron doped material, that is a manifestation of the cuprate superconductors ubiquitous tendency for d-wave superconducting order. Despite the strong differences between the p and n-type compounds in the larger scale electronic structure (~1 eV), their superconductivity appears to share the same symmetry and is therefore likely of similar origin.

Acknowledgements

This work was performed at the Stanford Synchrotron Radiation Laboratory which is supported by the DOE Office of Basic Energy Science, Divisions of Chemical Sciences and Material Sciences. It is also supported by the ONR grant N00014-98-1-0195 and NSF grant DMR-9705210. The crystal growth work was supported in part by Grant-in-Aids for Scientific Research from the Ministry of Education, Science, Sports, and Culture, Japan, and the New Energy and Industrial Technology Development Organization of Japan (NEDO).

References

[1] Y. Tokura et al., Nature 337 (1989) 345.
[2] F. Gollnik et al., Phys. Rev. B 58 (1998) 11734.
[3] Z. Wang et al., Phys. Rev. B 43 (1991) 3020.
[4] S. Kubo et al., Physica C 185–189 (1991) 1251.
[5] W. Jiang et al., Phys. Rev. Lett. 173 (1994) 1291.
[6] K. Thurston et al., Phys. Rev. Lett. 65 (1990) 263.
[7] K. Yamada, J. Phys. Chem. Solids 43 (1999) 1025.
[8] B. Stadlober et al., Phys. Rev. Lett. 74 (1995) 4911–4914.
[9] Q. Huang et al., Nature 347 (1990) 369–372.
[10] E.-J. Choi et al., Phys. Rev. B 53 (1996) R8859–R8862.
[11] D. Wu et al., Phys. Rev. Lett. 70 (1993) 85–88.
[12] S.H. Wang et al., Phys. Rev. Lett. 64 (1990) 1067–1070.
[13] C.C. Tsuei, J.R. Kirtley, cond-mat/0002341
[14] L. Alff et al., Phys. Rev. B 58 (1998) 11197–11200.
[15] S. Kashiwaya et al., Phys. Rev. B 57 (1998) 8680–8686.
[16] Z.-X. Shen, D.S. Dessau, Phys. Rep. 253 (1995) 1.
[17] D. King et al., Phys. Rev. Lett. 70 (1993) 3159.
[18] R.O. Anderson et al., Phys. Rev. Lett. 70 (1993) 3163.
[19] A. Schultz et al, Phys. Rev. B 53 (1996) 5157.
[20] A. Loeser et al., Phys. Rev. B 56 (1997) 14185.
[21] T. Yoshida et al., manuscript in preparation
[22] M. Schabel et al., Phys. Rev. B 55 (1997) 2796.
[23] N.P. Armitage et al., Nature, submitted.